Title: Ctenophore extracellular DNA traps demonstrate conserved antimicrobial behaviors present at the emergence of animals

Authors and Affiliations: Lauren E. Vandepas[a,b,c,e*†], Caroline Stefani[c†], Nikki Traylor-Knowles[d], Frederick W. Goetz[b], William E. Browne[e], Adam Lacy-Hulbert[c]
[a]NRC Research Associateship Program; [b]Northwest Fisheries Science Center, National Oceanographic and Atmospheric Administration, Seattle, WA 98112; [c]Benaroya Research Institute at Virginia Mason, Seattle, WA 98101; [d]University of Miami Rosenstiel School of Marine and Atmospheric Sciences, Miami, FL 33149; [e]University of Miami Department of Biology, Coral Gables, FL 33146; *Corresponding author; [†]Equal contribution

Key Words: *Ctenophore; ETosis; immune cell evolution;* Crassostrea gigas*; extracellular DNA traps*
Subject Areas: Immunology and Inflammation; Evolutionary Biology

Abstract

The formation of extracellular DNA traps (ETosis) is a first response mechanism by specific immune cells following exposure to microbes [1,2]. First characterized in vertebrate neutrophils, cells capable of ETosis have been recently discovered in several invertebrate taxa and the formation of invertebrate DNA traps has been most thoroughly examined in bivalves [3-5]. Here we report that ctenophores – thought to have diverged very early from the metazoan stem lineage [6,7] – possess immune cell types capable of ETosis, suggesting that this cellular immune response behavior was likely present early in metazoan evolution. To assess conservation of ET activation between evolutionarily distant phyla, we deployed a comparative approach integrating data from the model ctenophore *Mnemiopsis leidyi* and the oyster *Crassostrea gigas* to develop a novel imaging analysis pipeline to quantify ETosis in large numbers of cells. We demonstrate that both *Mnemiopsis* and *Crassostrea* immune cells can undergo ETosis after exposure to diverse microbes and pharmacological stimuli. Our results suggest that the range of cellular immune behaviors and signaling cascades that produce extracellular DNA traps were likely present prior to the divergence of extant metazoan lineages and thus ETosis represents an evolutionarily ancient defense against pathogens existing at the dawn of animal multicellularity.

Main

The release of extracellular DNA traps (ETs) is a morphologically and molecularly distinct immune-based process of cell death during which ETosis-competent immune cells cast nuclear chromatin material into the surrounding extracellular space in filamentous nets, trapping and killing invading microbes [8,9]. ETosis can be initiated by activation of specific signaling cascades following exposure to cytokines, microbes, pathogen-associated molecular patterns (PAMPs), or pharmacological agents [10,11]. Initially believed to be a behavior exclusive to vertebrate immune cells, a number of recent studies have highlighted ETosis as an anti-microbial behavior also present in non-vertebrate taxa [3,4,12-15]. Importantly, it remains unknown whether non-vertebrate immune cells competent for ETosis function via conserved molecular pathways. Thus the homology of non-vertebrate anti-microbial behavior to vertebrate leukocyte ETosis is unclear [15].

Prior to the production of ETs in vertebrate and bivalve mollusc immune cells, a reactive oxygen species (ROS) burst is required to activate signaling cascades (reviewed in Auguste et al 2020). Critically, ROS production can be generated through several distinct pathways depending on the stimulus [9]. For example, NADPH-dependent ETosis involves NOX (NADPH-

oxidase) generated by the plasma membrane, protein kinase C (PKC), and calcium, resulting in increased cytosolic ROS production following incubation with phorbol 12-myristate 13-acetate (PMA), fungi, or gram-positive bacteria, [10]. Alternatively, ETosis can be induced via a ROS burst from mitochondria independent of NOX [9,10,16,17]. Induction of ETosis can also be triggered through initiation of a calcium flux across the membrane in ETosis-competent cells via exposure to the calcium ionophore A23187, the potassium ionophore nigericin, or UV light [10,16]. Notably, induction of ETosis using calcium ionophores has been tested in relatively few taxa, and the stimulation of ETosis via the potassium ionophore nigericin has not been tested outside of vertebrate model systems.

Ctenophores (also known as "comb jellies") are a phylum of gelatinous planktonic marine invertebrates that diverge very early from the animal stem lineage and may represent the most ancient extant metazoan phylum [6,7]. Ctenophores have two distinct germ layers – ectoderm and endomesoderm – separated by a jelly-like layer of collagenous mesoglea, and lack a circulatory system where immune cells are typically concentrated (Fig. 1A). Understanding functional attributes of ctenophore physiological systems has provided insights into fundamental conservation of animal cell types and signaling pathways, as well as revealing mechanisms for emergence of evolutionary novelties [18-21]. Currently, the ctenophore immune system remains almost entirely undescribed [20,22].

Specific immune cell types have not been explicitly identified in ctenophores, though they do possess mobile amoebocyte-like or stellate cells that reside in the mesoglea and are capable of phagocytosis [20,23]. Whether ctenophores have other specialized mechanisms of cellular immune defense when exposed to classic microbial PAMPs has not been reported. Here we demonstrate that the model ctenophore *Mnemiopsis leidyi* possesses cell types capable of ETosis. Using a comparative approach with the oyster *Crassostrea gigas,* we further show in both distantly related species that ETosis is initiated in response to diverse microbial and pharmacological stimuli. To quantify the ETosis response, we developed a novel unbiased automated imaging pipeline to functionally identify and compare ETotic cells between species. Our data suggest that cellular immune behaviors and signaling cascades that trigger ETs under a range of stimuli represent an evolutionarily ancient defense against pathogens that was likely present prior to the divergence of extant metazoan lineages.

Results

Ctenophore immune cells undergo ETosis in response to pathogen exposure

To assess cellular immune responses to microbial challenge *in vitro*, we isolated live cells from whole ctenophore preparations (Fig. 1B). After incubation with fluorescent *Escherichia coli*, we observed motile, stellate cells competent for phagocytosing large amounts of bacteria (Supp. Video 1; Supp. Fig. 1). We further observed that some stellate cells changed their morphology dramatically by retracting their processes, undergoing nuclear rotation, and subsequently rapidly extruding nuclear material (Fig. 1C; Supp. Video 2). This behavior is remarkably similar to that of vertebrate monocytes during the cytoskeletal rearrangements preceding extracellular DNA trap (ET) formation [10,24]. This led us to speculate that some ctenophore immune cells were producing ETs in response to the presence of microbes.

We examined microbially-challenged *Mnemiopsis* cells using confocal microscopy and observed cells with decondensed DNA cast in large areas surrounding individual cell bodies. These networks of extracellular DNA were closely associated with individual *E. coli* (Fig. 1D). Three-dimensional rendering of confocal z-stacks revealed that *E. coli* bacteria were entangled in the extruded *Mnemiopsis* DNA (Fig. 1E; Supp. Video 3). To further characterize the extruded DNA using immunofluorescence, we stained cells with an antibody that recognizes an array of histone proteins (H1, H2A, H2B, H3, H4). We observed that *Mnemiopsis* immune cell ETs are composed of chromatin, typical of ETs described in other taxa (Fig. 1F). ETotic cells show

diffuse staining over a large area, whereas non-ETotic cells display intact nuclei with stereotypical complements of concentrated DNA and histone labeling (Fig. 1D-F; [9]). These data identify specific ctenophore cell types that produce *bona fide* extracellular chromatin traps when exposed to a microbial signature.

Diverse microbial signatures induce ET formation in *Mnemiopsis leidyi* independently of Non-ETotic cell death

To simultaneously and accurately quantify ETosis and non-ETotic cell death we developed a semi-automated imaging pipeline using a combination of two DNA dyes: Hoechst, a membrane-permeable stain which labels all cell nuclei, and SytoxGreen, a non-permeable stain, which selectively labels nuclei of dying or dead cells with compromised cell membranes. Both dyes label extracellular DNA nets (Fig. 2). Importantly, the nuclear envelopes of necrotic and apoptotic cells remain relatively intact, displaying concentrated fluorescent labeling [25]. Using our novel image analysis pipeline, we performed automated comparisons of thousands of images to accurately calculate percentages of live, dead, or ETotic cells. Critically, the development of this pipeline allowed us to accurately identify and discriminate between ETosis and non-ETotic cell death following treatments.

After exposing isolated *Mnemiopsis* cells to *E. coli* (Fig. 2A, B), we analyzed the stained nuclei in each image. Using image segmentation analysis, we defined individual cell masks based on Hoechst signal and measured relative fluorescence intensities of Hoechst and SytoxGreen inside each cell mask (Fig. 2C). Using those measurements, we defined 3 distinct cell populations: live cells, ETotic cells and non-ETotic cell death (Fig. 2D). Live cells are negative for SytoxGreen fluorescence with no dispersion of Hoechst signals ($Hoechst^{high}/SytoxGreen^{low}$) (Fig. 2B, 2D). Cells that have ETotic nuclei exhibit high dispersion of Hoechst fluorescence associated with extracellular DNA net formation ($Hoechst^{low}$). In contrast, cells that have condensed Hoechst fluorescence and high SytoxGreen fluorescent signals ($Hoechst^{high}/SytoxGreen^{high}$) are dying from non-ETotic cell death processes.This approach allowed us to accurately identify and quantify large numbers of cells, including those undergoing ETosis after incubation with *E. coli*.

We then expanded our analyses of ET production to include responses to additional microbial stimuli (https://github.com/carolinestefani/ETosis-and-death-automated-pipeline). We examined whether *Mnemiopsis* immune cells undergo ETosis when exposed to a diverse array of microbes, including the following: heat-killed gram-negative bacteria *E. coli*, heat-killed gram-positive bacteria *Staphylococcus aureus*, and cell wall extract from yeast *Saccharomyces cerevisiae* (zymosan). ETotic cells display diffuse Hoechst signal characteristic of filamentous DNA nets following exposure to *E. coli, S. aureus,* or zymosan (Fig. 3A). In contrast non-ETotic cells maintain intact nuclear material with concentrated Hoechst labeling. We analyzed both ETosis and total cell death in *Mnemiopsis* cells after four hours of microbial exposure (N=24 individual animals). Contour plots representing Hoechst and SytoxGreen signal intensities show three distinct clusters: ETotic cells, dying cells, and living cells (Fig. 3B).

ETosis events significantly increased in *Mnemiopsis* cells when exposed to zymosan or *E. coli in vitro*, with mean increases in detected ETotic events of 17% and 7% over untreated cells (Fig. 3C). Incubation with *S. aureus* also elicited a strong ETotic response in *Mnemiopsis* cells, with a mean increase in detected ETotic events of 69% over untreated cells. Notably, non-ETotic cell death increased significantly after incubation with *E. coli* but did not change after exposure to zymosan or *S. aureus* (Fig. 3C). Our data demonstrate that a panel of microbes stimulates ETosis in ctenophore cells and that we can accurately and efficiently measure Etosis and non-ETotic cell death events simultaneously.

Extracellular trap formation in *Mnemiopsis* is induced by classic pharmacological stimuli

ETosis can be induced in vertebrate granulocytes and leukocytes with pharmacological

agents that activate production of ROS via discrete intracellular signaling pathways [10,11,16]. Though ctenophore genomes appear to lack predicted gene homologs to many classic innate immunity pathway cell surface receptors and signaling intermediaries, many components of metazoan stress response pathways, as well as secondary messenger machinery, are present [20,26,27]. We hypothesized that ETosis in *Mnemiopsis* immune cells could be stimulated by classic chemical agents broadly used in studies of vertebrate ETs.

We observed a significant induction of ETosis in *Mnemiopsis* after a four-hour exposure to PMA, with a mean increase of 4.3% over untreated control cells (Fig. 3D-F). Nigericin, a potassium ionophore, induces ET formation in vertebrates by initiating ROS release from mitochondria (Kenny et al 2017; Meirer et al 2019). Initiation of a calcium influx following stimulation by calcium ionophore A23817 (calcimycin) can also induce ET formation independent of NOX (Douda et al 2015). We observed a significant induction of ETosis following incubation of *Mnemiopsis* cells with both the potassium ionophore nigericin and the calcium ionophore A23187, with a mean increase of 33% and 20% over untreated control cells, respectively (Fig. 3D-F). Nigericin exposure elicited the highest amount of ET formation (Fig. 3F; Supp. Video 4; Supp. Fig. 2).

While we did not observe a significant change in levels of non-ETotic cell death following PMA stimulus, our results did indicate a significant increase in non-ETotic cell death following nigericin and A23187 treatments (Fig. 3F). Exposure of *Mnemiopsis* cells to all three classical pharmacological stimuli – PMA, the potassium ionophore nigericin, and the calcium ionophore A23187 – induced significant ET formation. These results implicate diverse signaling pathways involved in production of ETs that also retain deep evolutionary conservation across extant metazoan phyla.

ETosis in the model bivalve, *Crassostrea gigas*, is induced by diverse microbial and chemical stimuli

We sought another non-vertebrate model to assess conservation of ET formation across phyla because ET stimulation in *Mnemiopsis* immune cells is intriguingly similar to ETosis in mammalian systems. The formation of invertebrate extracellular DNA traps has been characterized most extensively in molluscs [3-5,13,28]. Bivalve molluscs, like the Pacific oyster *Crassostrea gigas*, have blood-like circulatory cells, collectively called hemocytes, that have immune functions [29]. However, prior attempts to stimulate production of ETs in oyster via exposure to pathogen signatures and PMA has varied between studies [5]. For example previous studies observed a robust ETotic response following challenge with *Vibrio,* a virulent bivalve pathogen, in oyster hemocytes [3], however the induction of ETosis with other microbes has been only modest or not observed in previous studies {Romero, 2020 #6. Thus, conservation of ET induction pathways in bivalves remains unclear [3-5].

We measured ETs and cell death in *Crassostrea* hemocytes after exposure to zymosan, *E. coli*, and *S. aureus* (Fig. 4A-D). We found that ETosis is significantly stimulated in hemocytes exposed to all three pathogens (Fig 4D; Supp. Fig. 3), with mean increases of 13%, 19%, and 22% over untreated hemocytes, respectively. Hemocyte non-ETotic cell death (apoptosis, necrosis) increased significantly with *E. coli* exposure but not for zymosan challenge (Fig. 4D).

We also assayed *Crassostrea* hemocytes for ET production after exposure to pharmacological reagents that engage distinct signaling pathways in vertebrate monocytes. We analyzed the behavior of *Crassostrea* hemocytes after four-hour incubation with PMA, the potassium ionophore nigericin, and the calcium ionophore A23187 (Fig. 4E). Exposure to PMA and the calcium ionophore A23187 induced significant ET production in isolated *Crassostrea* hemocytes (Fig. 4F, 4G). However, the potassium ionophore nigericin showed no significant induction (Fig. 4F, 4G). In contrast, a large proportion of *Crassostrea* hemocytes produce ETs after 4 hours of exposure to A23187, similar to prior studies [5].

Discussion

Identifying the core molecular mechanisms of immune cells and their evolutionary origins is critical for understanding both the evolution of metazoan immunity function and the evolution of multicellularity. Initially described in 2004 as a unique antimicrobial behavior of vertebrate neutrophils, cells capable of extracellular trap production have recently subsequently been discovered in multiple non-vertebrate bilaterian taxa [4,12,14]. Here we report that ctenophore immune cells are competent for ETosis in response to microbial challenge and assess potential mechanisms associated with ETosis pathway activation with well-characterized pharmacological reagents. ETosis in both the model ctenophore *Mnemiopsis leidyi* and the model oyster *Crassostrea gigas* is initiated after exposure to diverse microbial signatures as well as pharmaceutical compounds that are known to activate distinct signaling cascades in vertebrates.

Many non-vertebrates lack gene homologs for major proteins known to be essential for ETosis in vertebrate neutrophils, such as PAD4, neutrophil elastase, and pannexin-1. It is currently unknown what signaling molecules are necessary for ET formation in non-vertebrate taxa. While the involvement of NADPH *per se* has not been directly assessed in invertebrate ET production, there is strong evidence for the presence of multiple ETosis pathways that can be activated via stimulation with microbial signatures, parasites, PMA, A23187, and UV light [3-5,12-14]. Prior studies in bivalves conflict as to whether ETosis can be stimulated with the NADPH-dependent pathway stimulus, PMA, or with microbes commonly used in immunological studies [4,5]. Our results demonstrate that *Crassostrea* hemocytes produce ETs in response to stimulation by diverse PAMPs and distinct pharmacological reagents that, in vertebrate monocytes, engage both NADPH-dependent signaling (PMA stimulus) and NADPH-independent signaling (A23187 stimulus). Notably, *Crassostrea* hemocytes did not produce ETs following stimulation by the potassium ionophore nigericin, suggesting a potential loss of nigericin stimulating signal transduction in this mollusc species.

Prior to ET production *in vitro*, *Mnemiopsis* immune cells and *Crassostrea* hemocytes that underwent ETosis after exposure to *E. coli* did not seem to have phagocytosed bacteria in significant amounts. Intriguingly, we observed other motile cells that phagocytosed large amounts of bacteria without undergoing ETosis (Supp. Video 1, Supp. Video 5; Supp. Fig. 3). Our functional characterization of ETosis competent cells in both taxa suggest that future studies should address whether the ETosis-competent and the highly phagocytic non-ETotic cells represent discrete immune cell types in these non-vertebrate taxa. In contrast to vertebrate immune cell nuclear morphologies that correspond with discrete immune cell functions [30], there do not seem to be notable differences in nuclear morphologies in either *Crassostrea* hemocytes or *Mnemiopsis* cells.

Ctenophores, which diverged very early from the metazoan stem lineage, have not had specific immune cell antimicrobial behaviors described beyond phagocytosis [20,23]. We demonstrate that *Mnemiopsis leidyi* possesses cells functionally competent for ETosis in response to a range of pathogen challenges. The production of extracellular traps in *Mnemiopsis* suggests this immune cell type specific antimicrobial defense behavior was likely present very early in metazoan evolution (Figure 5). Our data further demonstrates that both *Mnemiopsis leidyi* and *Crassostrea gigas* immune cells are capable of ETosis via stimulation with pharmaceutical agents that, in vertebrate immune cells, differentially induce either NADPH-dependent or NADPH-independent pathways to activate ET production. These data suggest that ETosis is an ancient and fundamental immune cell defense behavior that is not only present among distantly related metazoans but is also triggered by similar mechanisms.

Methods

Animal maintenance

Laboratory cultures of *Mnemiopsis leidyi* were maintained as previously described (Presnell, 2021 #35). Adult *Mnemiopsis* cells were isolated following established protocols [20,31,32]. *Crassostrea gigas* were maintained under flowing seawater at approximately 13°C and hemolymph was extracted from the adductor muscle with a syringe. Cells from both taxa were maintained *in vitro* under sterile conditions in filtered seawater (FSW) + 1% penicillin/streptomycin.

PAMP stimulation and imaging

For stimulation and quantification of ETosis, cells were isolated from 24 individual animals, plated in 96 well plates, and exposed to pHrodo-*E. coli*, *Staphylococcus aureus*, zymosan particles (Sigma Aldrich), 25 uM nigericin (Thermo Fisher Scientific), 1 mg/mL PMA (Sigma Aldrich), or 4 uM A23187 (Sigma). Each experimental condition for each animal was performed in triplicate. Live cell staining was performed following (2) and live imaging was performed using a JuLI Stage (NanoEntek).

For immunofluorescence, ctenophore cells were prepared following [32,33] and labeled with mouse anti-histone H11-4 (EMD Millipore) and anti-mouse Alexa Fluor 488 (Thermo Fisher Scientific). The H11-4 histone antibody was selected because it recognizes histones H1, H2A/B, H3, and H4 proteins across diverse species. Cells were treated with Hoechst 33342 (Sigma Aldrich) and SytoxGreen (Invitrogen) for 20 min, before imaging at 20X on an automated imaging plate reader, Cytation 3 (Biotek, software Gen5 v4.2).

Automated image-based profiling

We analyzed over 28,000 total images from our experiments using CellProfiler (v4.1.3). Image quality was assessed by calculating a focus score using two classes Otsu thresholding method, weighted variance on 20x20 pixel measurements. We calculated and applied an illumination correction for each fluorescent channel (SytoxGreen and Hoechst) using a background illumination function of 50 pixels block size, without smoothing. Each corrected image was then segmented using a global robust background method (0.05-50), with a smoothing scale of 1.3488 and a correction factor of 0.89. Clumped objects were identified and split by shape. For each segmented object we measured the number and intensity of pixels in each fluorescent channel.

Each image and each segmented object, along with Metadata, were exported as csv files by experiment. R (v4.0.5) software with tidyverse (v1.3.1), dplyr (v1.0.7) and readr (v1.4.0) packages were then used to transform the datasets. Data from images and objects were merged, and measurements from individual images with a Focus Score <0.2 were removed from further analysis. This allowed us to identify and select only images that were in focus. Surface area, Hoechst intensity and SytoxGreen intensity per object (nucleus) and per individual animal were then imported into FlowJo (v10.8.0), and percentages of cells per delineated population (dead/dying cell, live cell, and ETotic cell) were calculated. Dying cells were gated using Hoechst Intensity >0.35 and SytoxGreen intensity >0.1; live cells were gated using Hoechst Intensity > 0.35 and SytoxGreen intensity < 0.1; and ETotic cells were gated using Hoechst Intensity < 0.35. Finally, percentages per individual animal surveyed were combined and tested for statistical significance using GraphPad Prism (v9.2.0). All statistical tests were performed using two-tailed unpaired student t-test *p<0.05, **p<0.01, ***p<0.001, ****p<0.0001.

Acknowledgements

The authors are grateful to Anna Bruchez and Rachel Prins for imaging support. This research was supported by the National Oceanographic and Atmospheric Administration, a National

Research Council Postdoctoral Fellowship to LEV, and the National Science Foundation under Grant No. 2013692. CS and ALH were supported by National Institutes of Health Grants R33AI119341 and R01GM102482.

Author contributions

Conceptualization, C.S. and L.E.V.; Methodology, L.E.V. and C.S.; Formal Analysis, C.S.; Investigation, L.E.V. and C.S.; Writing – Original Draft, L.E.V. and C.S.; Writing – Review & Editing, C.S., A.L.H., W.E.B., N.T.K., F.W.G., and L.E.V.; Funding Acquisition, A.L.H., W.E.B., N.T.K., F.W.G., and L.E.V.; Resources, A.L.H., W.E.B., and F.W.G.; Supervision, A.L.H., W.E.B., and F.W.G.

Competing interests

The authors declare no competing interests.

Figures and Figure Legends

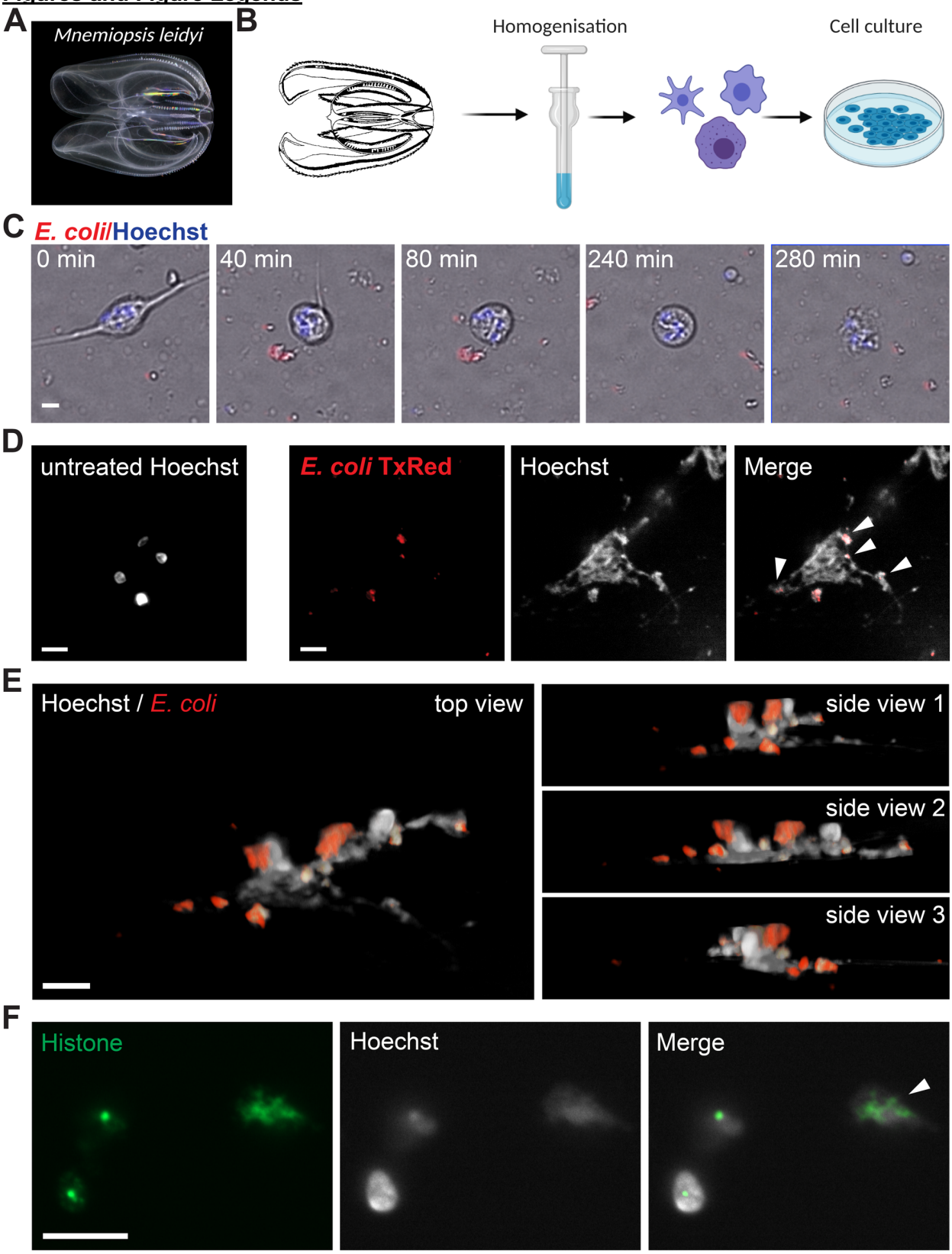

Figure 1. ***Mnemiopsis* immune cells produce extracellular DNA traps.** (A) Adult lobate ctenophore *Mnemiopsis leidyi*. (B) Schematic of isolation of cells from whole *Mnemiopsis leidyi*. (C) Still images from Movie S1 showing a motile stellate cell retracting its processes, spinning, and extruding its nuclear contents after exposure to *E. coli*. (D) Merged confocal image. Left – Nuclei of unstimulated *Mnemiopsis* cells. Right – A cell exposed to TxRed-*E. coli* has undergone ETosis; chromatin has been extruded from the cell in a large web-like pattern. *E. coli* are entrapped by the chromatin filaments (white arrowheads). (E) 3-dimensional image of *Mnemiopsis* extracellular DNA nets with *E. coli* entrapped. (F) Merged confocal image. Ctenophore extracellular traps are composed of DNA and histones. Histone 11-4 antibody (green) and Hoechst (white) staining are visible in intact and ETosed *Mnemiopsis* cells treated with the K+ ionophore nigericin. White arrowhead marks DNA+histone nets. (C-E scale bar: 10 µm).

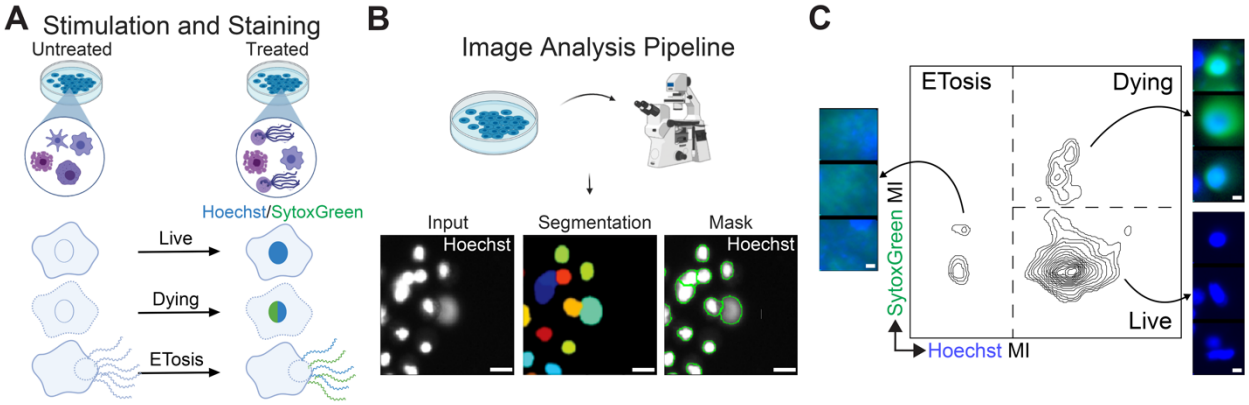

Figure 2. **Novel high-throughput imaging pipeline.** Schematic representation of experimental and imaging workflow. (A) Treated and untreated cells in culture were labeled with vital dye Hoechst and membrane impermeable Sytox Green and assessed for ETosis and/or cell death. (B) Example of the segmentation output and masking for identifying individual intact or ETosed nuclei. (C) Individual cells were scored for viability, ETosis, or death using FlowJo software. Scoring is based on fluorescent intensity and nuclear material area. Cells that have undergone ETosis exhibit dispersion and decreased intensity of Hoechst fluorescence associated with extracellular DNA net formation (Hoechst^{low}). In contrast, dead and dying cells have condensed Hoechst fluorescence and high SytoxGreen fluorescent signals (Hoechst^{high}/ SytoxGreen^{high}). High intensity blue fluorescence signals (Hoechst^{high}) denote intact nuclei of live cells.

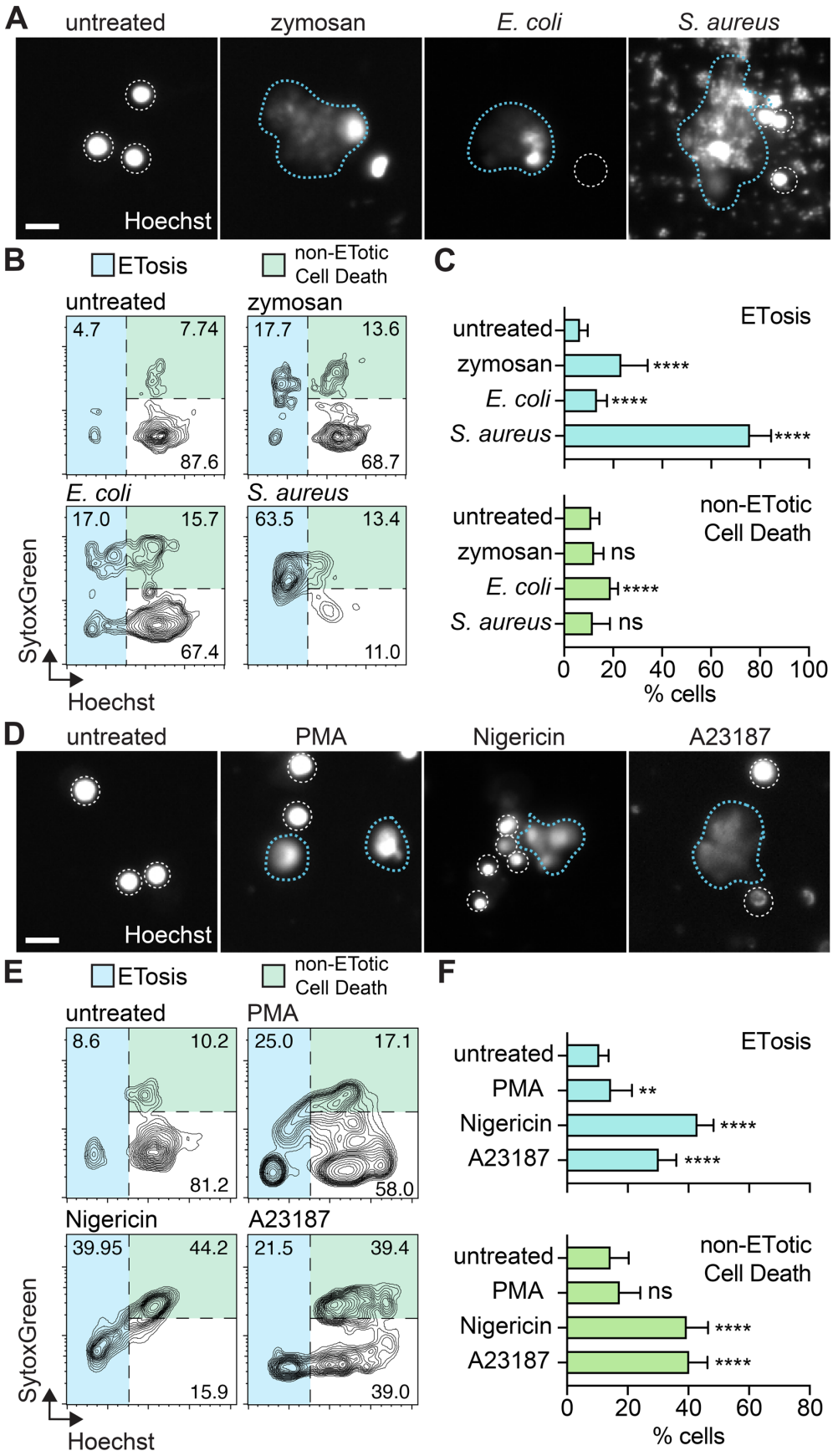
A
untreated
zymosan
E. coli
S. aureus
Hoechst
B
ETosis
non-ETotic Cell Death
untreated
zymosan
E. coli
S. aureus
4.7
7.74
87.6
17.7
13.6
68.7
17.0
15.7
67.4
63.5
13.4
11.0
SytoxGreen
Hoechst
C
ETosis
untreated
zymosan
E. coli
S. aureus
****
****
non-ETotic Cell Death
untreated
zymosan
E. coli
S. aureus
ns
****
ns
0
20
40
60
80
100
% cells
D
untreated
PMA
Nigericin
A23187
Hoechst
E
ETosis
non-ETotic Cell Death
untreated
PMA
Nigericin
A23187
8.6
10.2
81.2
25.0
17.1
58.0
39.95
44.2
15.9
21.5
39.4
39.0
SytoxGreen
Hoechst
F
ETosis
untreated
PMA
Nigericin
A23187
**
****
****
non-ETotic Cell Death
untreated
PMA
Nigericin
A23187
ns
****
****
0
20
40
60
80
% cells

Figure 3. **Diverse pathogen signatures and classic pharmaceuticals stimulate ETosis in *Mnemiopsis* immune cells.** (A) Representative images of ETotic *Mnemiopsis* cells exposed to fungal or bacterial pathogen signatures. (B) Representative FlowJo graph showing distributions of fluorescent signals from Hoechst and Sytox Green following pathogen exposures. (C) ETosis is significantly stimulated in *Mnemiopsis* cells exposed to zymosan, gram-negative *E. coli*, and gram-positive *S. aureus* after 4 hours. Apoptosis increases slightly with *E. coli* treatment but is not significant for other pathogen signatures. (D) Representative images of ETotic *Mnemiopsis* cells exposed to PMA, calcium ionophore A23187, or potassium ionophore nigericin. (E) Representative FlowJo graph showing distributions of fluorescent signals from Hoechst and Sytox Green following treatment with established ETosis-inducing pharmaceuticals. (F) ETosis is significantly stimulated in hemocytes exposed to PMA, nigericin, and A23187. Non-ETosis cell death increases significantly after incubation with ionophores nigericin and A23187, but not PMA.

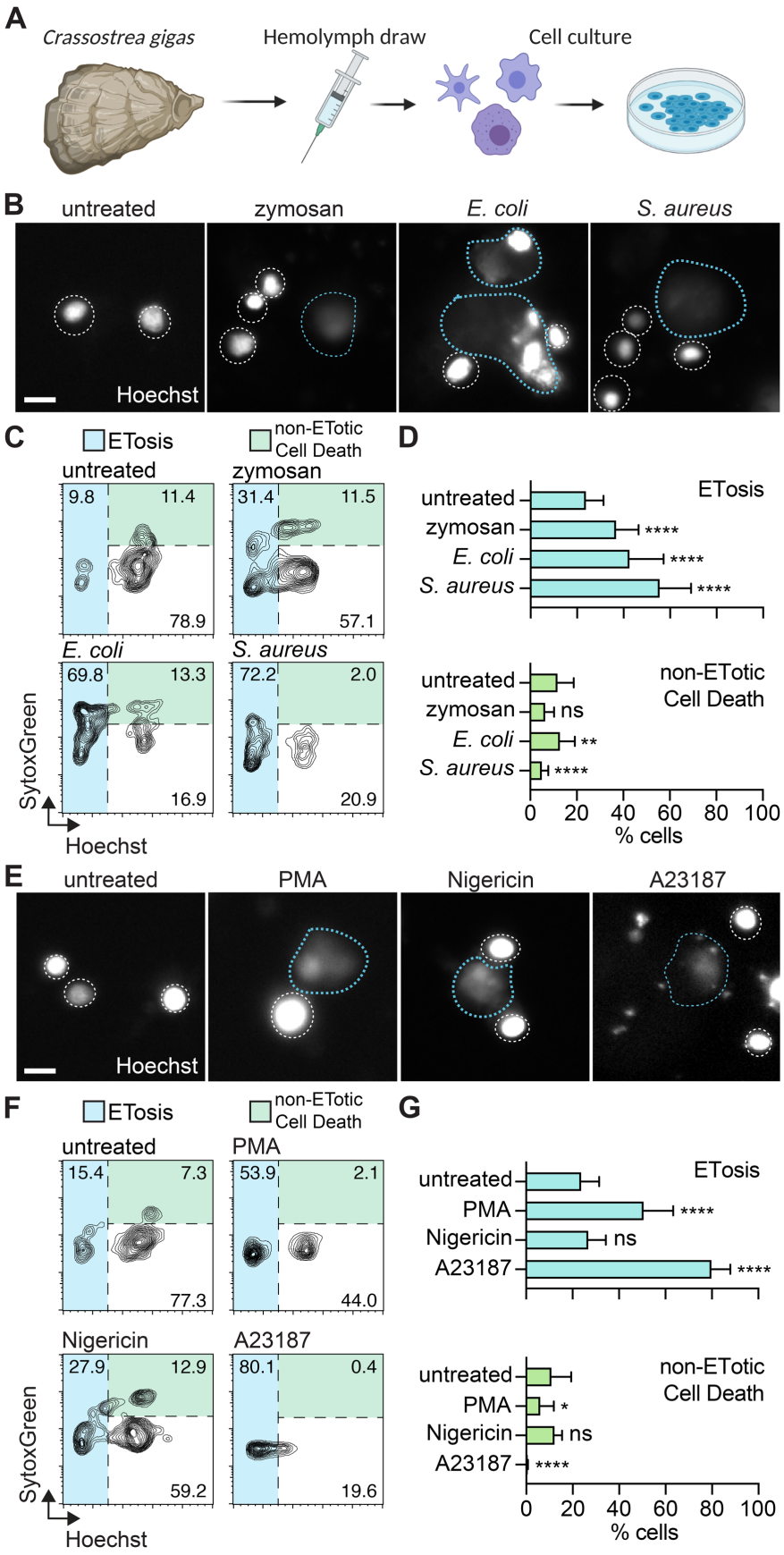
A
Crassostrea gigas
Hemolymph draw
Cell culture
B
untreated
zymosan
E. coli
S. aureus
Hoechst
C
ETosis
non-ETotic Cell Death
untreated
zymosan
E. coli
S. aureus
9.8
11.4
78.9
31.4
11.5
57.1
69.8
13.3
16.9
72.2
2.0
20.9
SytoxGreen
Hoechst
D
ETosis
untreated
zymosan
E. coli
S. aureus
****
****
****
non-ETotic Cell Death
ns
**
****
0
20
40
60
80
100
% cells
E
untreated
PMA
Nigericin
A23187
Hoechst
F
ETosis
non-ETotic Cell Death
untreated
PMA
Nigericin
A23187
15.4
7.3
77.3
53.9
2.1
44.0
27.9
12.9
59.2
80.1
0.4
19.6
SytoxGreen
Hoechst
G
ETosis
untreated
PMA
Nigericin
A23187
****
ns
****
non-ETotic Cell Death
*
ns
****
0
20
40
60
80
100
% cells

Figure 4. **Some pathogen signatures and classic pharmaceuticals induce ETosis in *Crassostrea* hemocytes.** (A) Schematic of hemocyte isolation from Pacific oyster *Crassostrea gigas.* (B) Representative images of ETotic *C. gigas* hemocytes exposed to fungal or bacterial pathogen signatures. PMA, calcium ionophore A23187, and potassium ionophore nigericin significantly induce ETosis in *Crassostrea* hemocytes. (C) Representative FlowJo graph showing distributions of fluorescent signals from Hoechst and Sytox Green following pathogen exposures. (D) ETosis is significantly stimulated in *Crassostrea* cells exposed to zymosan, gram-negative *E. coli*, and gram-positive *S. aureus* after 4 hours. Apoptosis increases slightly with *E. coli* treatment and decreases following *S. aureus* incubation, but is not significant for zymosan. (E) Representative images of ETotic *C. gigas* hemocytes stimulated with PMA, A23187, or nigericin. (F) Representative FlowJo graph showing distributions of fluorescent signals from Hoechst and Sytox Green following treatment with established ETosis-inducing pharmaceuticals. (G) PMA and A23187, but not nigericin, significantly stimulates ETosis in hemocytes. Apoptosis of hemocytes decreases when treated with PMA or A23187.

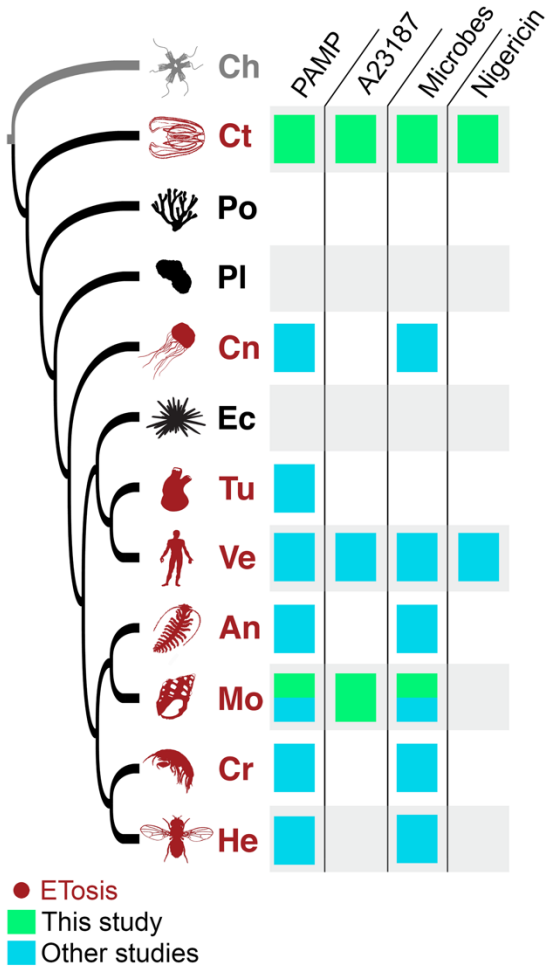

Figure 5. **ETosis is an ancient metazoan immune response.** Summary of ETosis phenomena across Metazoa. The presence of cells competent for ETosis in protostome, deuterostome, and non-bilaterian taxa indicate that production of extracellular DNA traps is an ancient animal immune defense.

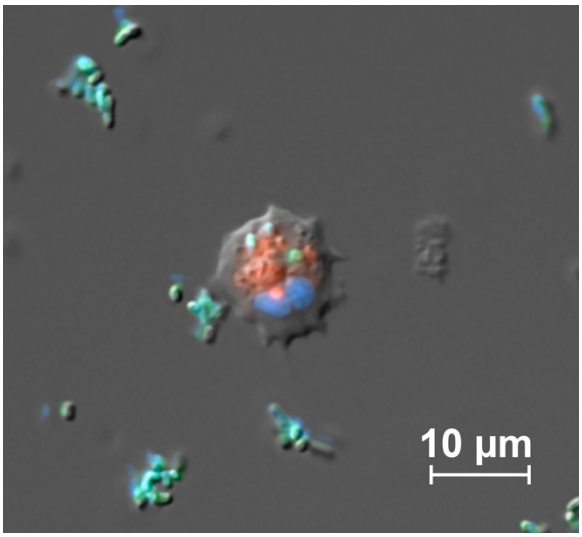

Supp. Figure 1: Merged brightfield and fluorescent image of a live *Mnemiopsis* motile, stellate cell that has phagocytosed fluorescent *E. coli* (green). Nuclei are labeled with Hoechst (blue). Lysosomes are labeled with Lysotracker-redDND99 (red). Scale bar is 10 µm.

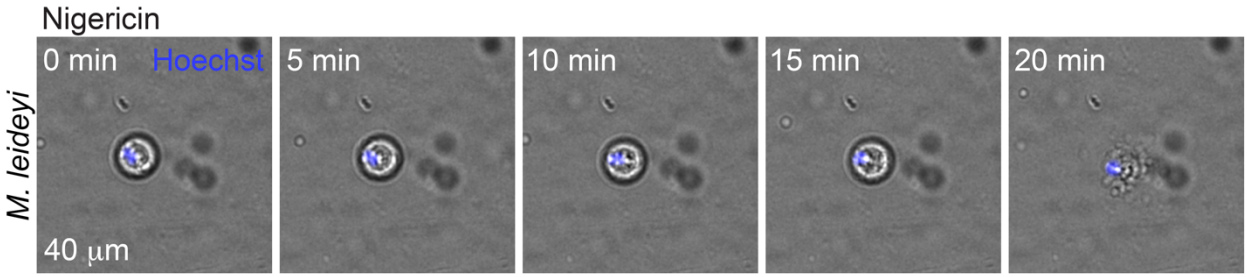

Supp. Figure 2: Merged brightfield and fluorescent images of video stills of a live *Mnemiopsis* motile, stellate cell undergoing ETosis following exposure to the K+ ionophore nigericin. Time stamps denote how long the expulsion of nuclear material occurs. Nuclei are labeled with Hoechst (blue).

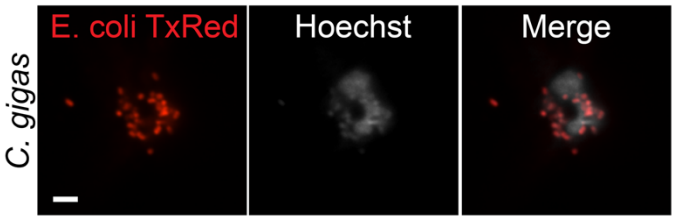

Supp. Figure 3: Confocal image of a *C. gigas* hemocyte that has undergone ETosis in response to exposure to Tx-red-*E. coli.* Individual bacteria are entangled in the expelled nuclear material. Scale bar is 5 µm.

C. gigas

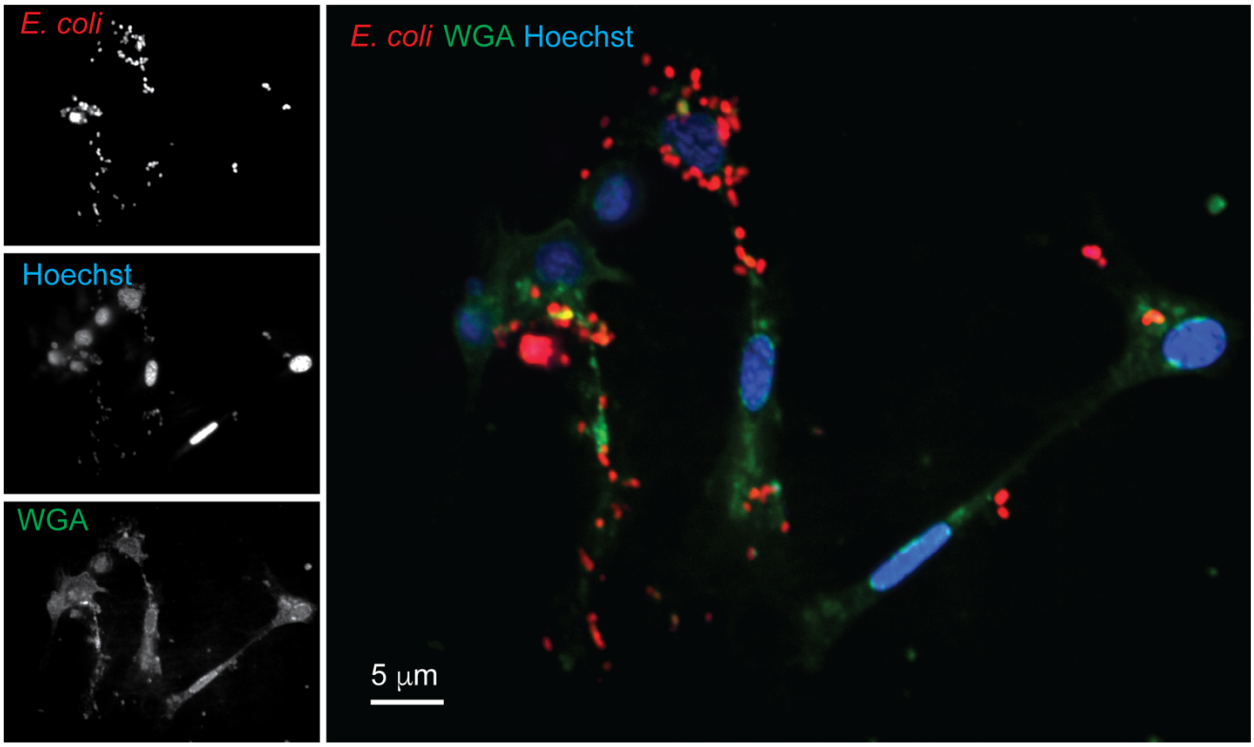

Supp. Figure 4: Confocal image of phagocytic *C. gigas* hemocytes that have engulfed Tx-red-labeled *E. coli.* Hemocyte cell membranes are labeled with WGA (green). Nuclei are labeled with Hoechst (blue). Scale bar is 5 µm.

Supp. Video 1: Merged brightfield and fluorescent video of a live *Mnemiopsis* motile, stellate cell that is phagocytosing fluorescent *E. coli* (green). Scale bar is 10 µm.

Supp. Video 2: Merged brightfield and fluorescent video of a live *Mnemiopsis* motile, stellate cell undergoing ETosis after *in vitro* exposure to pHrodo-*E. coli*. The cell moves into view, retracts its processes, spins, and exudes its nuclear material. DNA (Hoechst, blue), pHrodo-*E. coli* (red)

Supp. Video 3: 3D reconstruction of confocal stack of *Mnemiopsis* extracellular DNA traps. DNA (Hoechst, white) is extracellular, in filamentous “nets”; lysosomal marker (Lysotracker, green) denotes cellular debris; bacteria are ensnared in the “nets” (pHrodo-*E. coli*, red)

Supp. Video 4: Merged brightfield and fluorescent video of a live *Mnemiopsis* motile, stellate cell undergoing ETosis after *in vitro* exposure to K+ ionophore nigericin, which stimulates NADPH-independent ETosis. DNA (Hoechst, blue)

Supp. Video 5: Merged brightfield and fluorescent video of live *C. gigas* hemocytes phagocytosing Tx-Red-*E. coli*. Multiple cells ingest the bacteria and continue scavenging. Brightfield, pHrodo, *E. coli* (red)

References

1 Brinkmann, V. *et al.* Neutrophil extracellular traps kill bacteria. *Science* **303**, 1532-1535, doi:10.1126/science.1092385 (2004).

2 Wartha, F., Beiter, K., Normark, S. & Henriques-Normark, B. Neutrophil extracellular traps: casting the NET over pathogenesis. *Curr Opin Microbiol* **10**, 52-56, doi:10.1016/j.mib.2006.12.005 (2007).

3 Poirier, A. C. *et al.* Antimicrobial histones and DNA traps in invertebrate immunity: evidences in Crassostrea gigas. *J Biol Chem* **289**, 24821-24831, doi:10.1074/jbc.M114.576546 (2014).

4 Robb, C. T., Dyrynda, E. A., Gray, R. D., Rossi, A. G. & Smith, V. J. Invertebrate extracellular phagocyte traps show that chromatin is an ancient defence weapon. *Nat Commun* **5**, 4627, doi:10.1038/ncomms5627 (2014).

5 Romero, A., Novoa, B. & Figueras, A. Extracellular traps (ETosis) can be activated through NADPH-dependent and -independent mechanisms in bivalve mollusks. *Dev Comp Immunol* **106**, 103585, doi:10.1016/j.dci.2019.103585 (2020).

6 Dunn, C. W. *et al.* Broad phylogenomic sampling improves resolution of the animal tree of life. *Nature* **452**, 745-749, doi:10.1038/nature06614 (2008).

7 Li, Y., Shen, X. X., Evans, B., Dunn, C. W. & Rokas, A. Rooting the Animal Tree of Life. *Mol Biol Evol* **38**, 4322-4333, doi:10.1093/molbev/msab170 (2021).

8 Fuchs, T. A. *et al.* Novel cell death program leads to neutrophil extracellular traps. *J Cell Biol* **176**, 231-241, doi:10.1083/jcb.200606027 (2007).

9 Sollberger, G., Tilley, D. O. & Zychlinsky, A. Neutrophil Extracellular Traps: The Biology of Chromatin Externalization. *Dev Cell* **44**, 542-553, doi:10.1016/j.devcel.2018.01.019 (2018).

10 Kenny, E. F. *et al.* Diverse stimuli engage different neutrophil extracellular trap pathways. *Elife* **6**, doi:10.7554/eLife.24437 (2017).

11 Auguste, M., Balbi, T., Ciacci, C. & Canesi, L. Conservation of Cell Communication Systems in Invertebrate Host-Defence Mechanisms: Possible Role in Immunity and Disease. *Biology (Basel)* **9**, doi:10.3390/biology9080234 (2020).

12 Homa, J., Ortmann, W. & Kolaczkowska, E. Conservative Mechanisms of Extracellular Trap Formation by Annelida Eisenia andrei: Serine Protease Activity Requirement. *PLoS One* **11**, e0159031, doi:10.1371/journal.pone.0159031 (2016).

13 Lange, M. K. *et al.* Gastropod-derived haemocyte extracellular traps entrap metastrongyloid larval stages of Angiostrongylus vasorum, Aelurostrongylus abstrusus and Troglostrongylus brevior. *Parasit Vectors* **10**, 50, doi:10.1186/s13071-016-1961-z (2017).

14 Nascimento, M. T. C. *et al.* DNA extracellular traps are part of the immune repertoire of Periplaneta americana. *Dev Comp Immunol* **84**, 62-70, doi:10.1016/j.dci.2018.01.012 (2018).

15 Ramos-Martinez, E. *et al.* Multiple Origins of Extracellular DNA Traps. *Front Immunol* **12**, 621311, doi:10.3389/fimmu.2021.621311 (2021).

16 Douda, D. N., Khan, M. A., Grasemann, H. & Palaniyar, N. SK3 channel and mitochondrial ROS mediate NADPH oxidase-independent NETosis induced by calcium influx. *Proc Natl Acad Sci U S A* **112**, 2817-2822, doi:10.1073/pnas.1414055112 (2015).

17 Papayannopoulos, V. Neutrophil extracellular traps in immunity and disease. *Nat Rev Immunol* **18**, 134-147, doi:10.1038/nri.2017.105 (2018).

18 Babonis, L. S., Ryan, J. F., Enjolras, C. & Martindale, M. Q. Genomic analysis of the tryptome reveals molecular mechanisms of gland cell evolution. *Evodevo* **10**, 23, doi:10.1186/s13227-019-0138-1 (2019).

19 Jokura, K. *et al.* CTENO64 Is Required for Coordinated Paddling of Ciliary Comb Plate in Ctenophores. *Curr Biol* **29**, 3510-3516 e3514, doi:10.1016/j.cub.2019.08.059 (2019).

20 Traylor-Knowles, N., Vandepas, L. E. & Browne, W. E. Still Enigmatic: Innate Immunity in the Ctenophore Mnemiopsis leidyi. *Integr Comp Biol* **59**, 811-818, doi:10.1093/icb/icz116 (2019).
21 Presnell, J. S. & Browne, W. E. Kruppel-like factor gene function in the ctenophore Mnemiopsis leidyi assessed by CRISPR/Cas9-mediated genome editing. *Development* **148**, doi:10.1242/dev.199771 (2021).
22 Bolte, S. *et al.* Specific immune priming in the invasive ctenophore Mnemiopsis leidyi. *Biol Lett* **9**, 20130864, doi:10.1098/rsbl.2013.0864 (2013).
23 Franc, J. M. La matrice mésogléenne des Cténaires. *Bulletin de la Société zoologique de France* **113**, 347-447 (1988).
24 Boe, D. M., Curtis, B. J., Chen, M. M., Ippolito, J. A. & Kovacs, E. J. Extracellular traps and macrophages: new roles for the versatile phagocyte. *J Leukoc Biol* **97**, 1023-1035, doi:10.1189/jlb.4RI1014-521R (2015).
25 Guimaraes-Costa, A. B., Nascimento, M. T., Wardini, A. B., Pinto-da-Silva, L. H. & Saraiva, E. M. ETosis: A Microbicidal Mechanism beyond Cell Death. *J Parasitol Res* **2012**, 929743, doi:10.1155/2012/929743 (2012).
26 Ryan, J. F. *et al.* The genome of the ctenophore Mnemiopsis leidyi and its implications for cell type evolution. *Science* **342**, 1242592, doi:10.1126/science.1242592 (2013).
27 Moroz, L. L. *et al.* The ctenophore genome and the evolutionary origins of neural systems. *Nature* **510**, 109-114, doi:10.1038/nature13400 (2014).
28 Bachere, E. *et al.* The new insights into the oyster antimicrobial defense: Cellular, molecular and genetic view. *Fish Shellfish Immunol* **46**, 50-64, doi:10.1016/j.fsi.2015.02.040 (2015).
29 Jiang, S. *et al.* Functional characterisation of phagocytes in the Pacific oyster Crassostrea gigas. *PeerJ* **4**, e2590, doi:10.7717/peerj.2590 (2016).
30 Skinner, B. M. & Johnson, E. E. Nuclear morphologies: their diversity and functional relevance. *Chromosoma* **126**, 195-212, doi:10.1007/s00412-016-0614-5 (2017).
31 Presnell, J. S. *et al.* The Presence of a Functionally Tripartite Through-Gut in Ctenophora Has Implications for Metazoan Character Trait Evolution. *Curr Biol* **26**, 2814-2820, doi:10.1016/j.cub.2016.08.019 (2016).
32 Vandepas, L. E., Warren, K. J., Amemiya, C. T. & Browne, W. E. Establishing and maintaining primary cell cultures derived from the ctenophore Mnemiopsis leidyi. *J Exp Biol* **220**, 1197-1201, doi:10.1242/jeb.152371 (2017).
33 Acharya, M. *et al.* alphav Integrins combine with LC3 and atg5 to regulate Toll-like receptor signalling in B cells. *Nat Commun* **7**, 10917, doi:10.1038/ncomms10917 (2016).